

A Mathematical Model of Wasting–Stunting Dynamics with Age-Dependent Nutritional Recovery in Children under Five

Nur Rahmi^{1*}, Wahyuni Ekasasmita¹, Muhammad Rifki Nisardi¹, Ahmad Fajri¹,
Muhammad Fadhil Nurahmad¹, Hartina Husain¹, Ahmad Husain^{1,2}

¹Department of Science, Institut Teknologi Bacharuddin Jusuf Habibie, Indonesia

²Department of Production and Industrial Technology, Institut Teknologi Bacharuddin Jusuf Habibie,
Indonesia

nurrahmi@ith.ac.id

ABSTRACT

Article History:

Received : 09-04-2026
Revised : 18-05-2026
Accepted : 23-05-2026
Online : 01-07-2026

Keywords:

Age-dependent
Recovery;
Child Malnutrition;
Stunting-wasting;
Stability Analysis;
Sensitivity Analysis.



Childhood wasting and stunting remain major public health challenges, yet their long-term interaction at the population level remains insufficiently understood. This study develops a deterministic compartmental model to investigate wasting–stunting dynamics among children under five years of age in Indonesia by classifying the population into four nutritional states: well-nourished, moderately wasted, severely wasted, and stunted. An important feature of the model is the incorporation of age-dependent recovery weighting based on infant population proportion, allowing recovery rates to differ between infants and older children according to demographic composition. Model parameters are estimated using nonlinear least-squares calibration based on aggregated national prevalence data from Indonesia during 2013–2024. Concurrent wasting–stunting is incorporated implicitly within the stunting dynamics to maintain model parsimony. The analysis includes threshold, local stability, and normalized sensitivity analyses. The calibrated model produced a residual error of approximately 8.77×10^{-3} , indicating good agreement with observed prevalence data. Numerical simulations show declining and stabilizing behavior for severe wasting, whereas stunting remains persistent over time. Threshold analysis indicates that the condition $\mathcal{R}_w < 1$ is associated with decay of wasting dynamics and convergence toward equilibrium. Sensitivity analysis indicates that deterioration and progression toward stunting dominate long-term dynamics, while infant-related recovery parameters exhibit relatively low sensitivity rankings. These findings suggest that reducing wasting alone may not substantially lower stunting prevalence and highlight the importance of integrated interventions targeting both acute and chronic undernutrition pathways.



<https://doi.org/10.31764/jtam.v10i3.39083>



This is an open access article under the **CC-BY-SA** license

A. INTRODUCTION

Child malnutrition remains one of the most persistent global public health challenges, with profound long-term consequences for physical growth, cognitive development, educational attainment, and survival. According to recent global estimates, approximately 150.2 million children under five years of age were affected by stunting in 2024, reflecting the continuing burden of chronic undernutrition worldwide (UNICEF/WHO/World Bank Group, 2025). Stunting is associated with impaired linear growth, delayed neurocognitive development, weakened immune function, increased susceptibility to infectious diseases, and elevated long-term health vulnerability (Harper et al., 2023; Indahsari et al., 2023; Masitoh et al., 2023; Murni

et al., 2023; Nomura et al., 2023; Wicaksono et al., 2021). Beyond its biological consequences, childhood undernutrition also contributes to substantial socioeconomic losses through reduced educational achievement, lower workforce productivity, and increased healthcare expenditures, thereby hindering sustainable national development (Meisel et al., 2018).

Among the major forms of child undernutrition, wasting and stunting have traditionally been studied as distinct nutritional conditions representing acute and chronic manifestations of malnutrition, respectively. However, increasing empirical evidence suggests that these conditions are strongly interconnected rather than biologically independent. Several longitudinal and pooled analyses have demonstrated that children experiencing wasting face substantially higher risks of subsequent stunting, particularly during critical periods of early childhood growth (Jokhu & Syauqy, 2024; Mertens et al., 2023; Schoenbuchner et al., 2019). Recurrent or prolonged wasting episodes may impair linear growth through metabolic stress, micronutrient deficiencies, inflammatory responses, and repeated infections, thereby increasing vulnerability to chronic growth failure. Conversely, children affected by chronic stunting may also exhibit weakened physiological resilience, making them more susceptible to subsequent acute wasting episodes. These findings indicate that wasting and stunting should not be interpreted as isolated nutritional outcomes, but rather as interacting processes within a broader continuum of undernutrition.

Despite the growing recognition of wasting–stunting interactions at the individual level, their long-term implications at the population level remain insufficiently understood. In particular, it is still unclear whether reducing wasting prevalence alone is sufficient to substantially reduce long-term stunting prevalence, or whether chronic undernutrition may persist even after acute malnutrition declines. This issue is highly relevant from a public health perspective because many nutritional intervention programs focus primarily on short-term wasting treatment without fully addressing the structural determinants of chronic growth failure. Consequently, understanding how wasting progression, recovery dynamics, and direct pathways toward stunting interact over time remains an important unresolved problem in child nutrition research.

Child malnutrition itself is shaped by multiple interconnected determinants operating across biological, environmental, and socioeconomic dimensions (Aisyah et al., 2024; Hamid et al., 2024; K. M. Harper et al., 2018). Poor infant feeding practices, recurrent infections, inadequate sanitation, household food insecurity, maternal malnutrition, and limited healthcare access all contribute to both acute and chronic undernutrition (Bahagia Febriani et al., 2020; Fikri & Komalyna, 2023; Masitoh et al., 2023; Millward, 2017; Permatasari et al., 2024; Singh et al., 2014). In Indonesia and other low- and middle-income settings, disparities in maternal education, healthcare accessibility, and environmental sanitation further exacerbate child nutritional vulnerability (Aisyah et al., 2024; Damanik et al., 2025; Indahsari et al., 2023; Tello et al., 2022). These determinants interact through complex and nonlinear pathways, making long-term nutritional dynamics difficult to evaluate using conventional statistical approaches alone.

Importantly, recovery from malnutrition is also known to vary substantially across age groups. Infants below one year of age generally exhibit greater physiological plasticity, faster growth responsiveness, and higher recovery potential following nutritional interventions

compared with older children, particularly during the critical first 1000 days of life (Mertens et al., 2023). Nutritional rehabilitation during infancy is therefore often more effective than interventions implemented at later ages, when chronic growth deficits become increasingly difficult to reverse. Nevertheless, age-dependent recovery mechanisms remain largely neglected in existing mathematical models of childhood undernutrition. Most available compartmental frameworks assume homogeneous recovery rates across all children under five, thereby overlooking demographic heterogeneity that may substantially influence long-term nutritional trajectories.

Mathematical modeling provides a powerful analytical framework for investigating such complex systems because it enables the representation of nonlinear interactions, competing nutritional pathways, and long-term temporal dynamics within a unified structure (Rahmi & Ekasasmita, 2024). Existing mathematical studies on malnutrition, however, remain limited in several important aspects. Many previous models adopt epidemiological SEIR-type formulations Avalos et al. (2021); Himmah et al. (2025); Winarni et al. (2024) implicitly treating malnutrition states analogously to infectious disease compartments rather than as progressive and partially reversible nutritional conditions. Moreover, most previous studies focus on a single form of malnutrition, either wasting or stunting, without explicitly modeling the interaction pathways linking acute and chronic undernutrition. Existing works also rarely integrate empirical calibration, threshold analysis, and sensitivity analysis simultaneously, limiting quantitative interpretation of the relative importance of competing nutritional mechanisms.

Another important limitation concerns concurrent wasting–stunting. Although concurrent malnutrition is clinically important due to its elevated mortality risk (Mertens et al., 2023), longitudinal population-level data describing concurrent nutritional trajectories remain highly limited. Consequently, many previous studies either neglect concurrent conditions entirely or require highly complex model structures that are difficult to calibrate reliably using aggregated prevalence data. These limitations motivate the need for parsimonious yet biologically interpretable frameworks capable of integrating available epidemiological information without excessive model complexity.

To address these gaps, this study develops a deterministic compartmental model describing childhood undernutrition dynamics through four interacting nutritional states: well-nourished, moderately wasted, severely wasted, and stunted. Unlike classical compartmental epidemic models, the proposed framework focuses specifically on undernutrition interactions rather than infectious disease transmission processes. The model incorporates both wasting-mediated progression and direct pathways toward stunting, thereby enabling simultaneous representation of acute and chronic nutritional deterioration.

The primary novelty of this study lies in the incorporation of age-dependent recovery dynamics through a time-varying demographic weighting mechanism based on the proportion of infants within the under-five population. In the proposed framework, recovery rates are not assumed homogeneous across all children. Instead, infants aged below one year are assumed to recover more rapidly than older children due to higher biological plasticity and stronger responsiveness to nutritional interventions. This mechanism enables the model to explicitly capture demographic heterogeneity in recovery behavior, thereby providing a more

biologically realistic representation of child undernutrition dynamics. To the best of our knowledge, relatively few previous mathematical models of wasting–stunting interactions have explicitly incorporated infant-sensitive recovery dynamics within a calibrated population-level framework.

To maintain model identifiability and consistency with available national-level prevalence data, concurrent wasting–stunting is not introduced as a separate compartment. Instead, concurrent undernutrition is represented implicitly within the stunting dynamics as overlapping nutritional conditions. This approach preserves model parsimony while remaining consistent with the limitations of aggregated demographic and nutritional surveillance data. Model parameters are estimated using nonlinear least-squares calibration against observed prevalence data, while nondimensional analysis, threshold analysis, and local stability analysis are employed to investigate the qualitative behavior of the system. In addition, sensitivity analysis is performed to identify the dominant parameters governing long-term undernutrition dynamics and to evaluate the relative influence of deterioration and recovery pathways.

By integrating mechanistic modeling, demographic heterogeneity, age-dependent recovery dynamics, empirical calibration, and sensitivity analysis within a unified framework, this study provides new insight into the persistence of chronic undernutrition and the relative contribution of wasting dynamics to long-term stunting prevalence. The findings are expected to support more integrated nutritional intervention strategies that simultaneously address acute wasting management and long-term stunting prevention.

B. METHODS

1. Research Framework

This study applies a quantitative mathematical modeling approach to investigate the dynamics of wasting and stunting among children under five years of age in Indonesia. The research process began with problem identification and literature review, followed by formulation of model assumptions, development of the mathematical model, theoretical analysis, parameter calibration, sensitivity analysis, and numerical simulation. The overall research procedure is summarized in Figure 1.

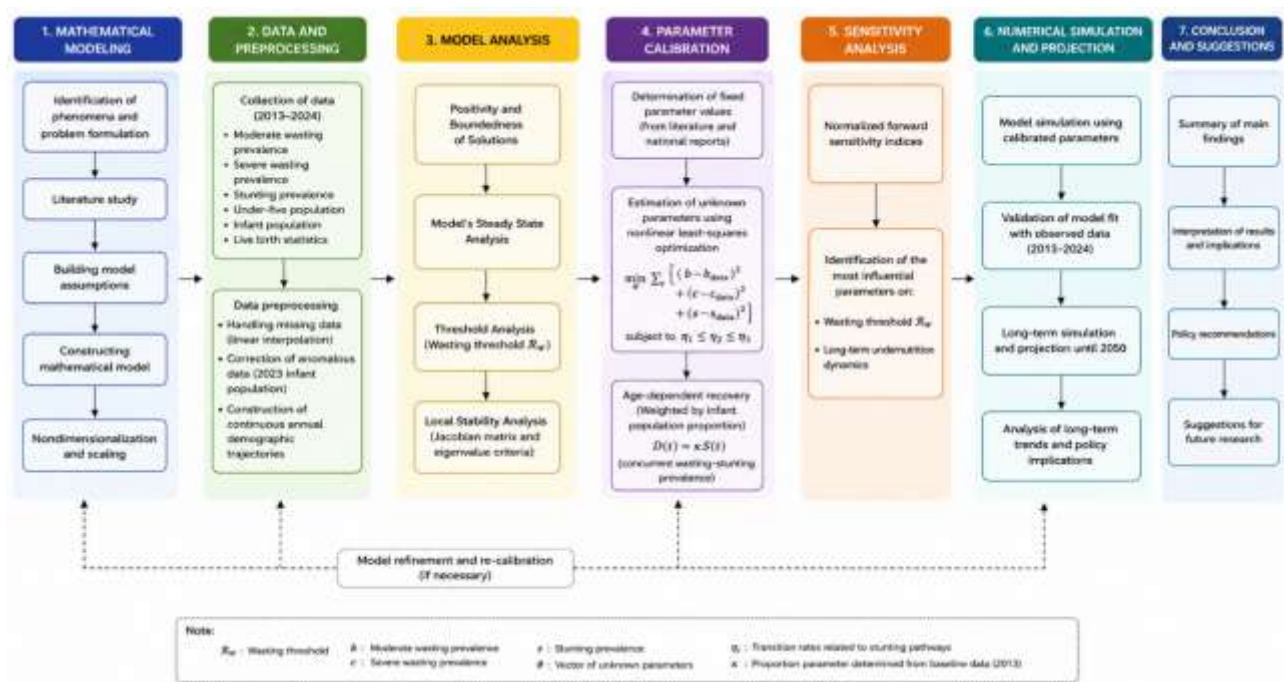


Figure 1. Methodological procedures

2. Data Preprocessing

The study employed aggregated national demographic and nutritional prevalence data in Indonesia during 2013–2024, including moderate wasting prevalence, severe wasting prevalence, stunting prevalence, under-five population, infant population, and live birth statistics (Badan Kebijakan Pembangunan Kesehatan (BKPK) Kementerian Kesehatan Republik Indonesia, 2024; Badan Penelitian dan Pengembangan Kesehatan, 2019; Kementerian Kesehatan Republik Indonesia, 2025a, 2025b, 2013, 2016, 2017, 2018, 2019, 2022, 2023, 2024).

Prior to calibration and simulation, preprocessing procedures were performed to ensure temporal consistency and biological plausibility of the dataset. Missing demographic observations were reconstructed using linear interpolation to obtain continuous annual demographic trajectories within the simulation framework. In addition, the infant population data for 2023 exhibited an anomalously high value relative to neighboring years, producing an unrealistic demographic proportion. This outlier was corrected through interpolation using adjacent observations to preserve biologically realistic demographic patterns throughout the simulation period.

3. Parameter Calibration

Several parameter values were determined from literature and available national reports, whereas unknown parameters were estimated using nonlinear least-squares optimization by fitting the dimensional form of the model to observed prevalence data of moderate wasting, severe wasting, and stunting. The calibration procedure minimized discrepancies between simulated and observed prevalence trajectories while imposing biologically motivated constraints on progression pathways toward stunting. The optimization was implemented using MATLAB's `\texttt{lsqnonlin}` function based on the Levenberg–Marquardt algorithm.

To incorporate demographic heterogeneity in recovery dynamics, recovery parameters were formulated using infant population weighting, allowing recovery rates to differ between infants and older children according to annual demographic composition. In addition, concurrent wasting–stunting prevalence was incorporated indirectly as a derived proportion of the stunting population to maintain model parsimony and consistency with available prevalence data. The dimensional form of the model was employed during calibration because it preserves the biological interpretation of transition and recovery rates while providing greater flexibility for fitting temporally varying prevalence data. The detailed calibration formulation and estimated parameter values are presented in the subsequent results section.

4. Sensitivity Analysis and Numerical Simulation

Sensitivity analysis was conducted to evaluate the relative influence of model parameters on long-term undernutrition dynamics and the wasting threshold. The analysis employed normalized forward sensitivity indices based on the standardized form of the model, allowing direct comparison of parameter influence within a dimensionless framework. Parameters associated with deterioration, progression, and recovery pathways were systematically perturbed to assess their relative contribution to system behavior.

Numerical simulations were subsequently performed using the calibrated parameter set to investigate the temporal dynamics of moderate wasting, severe wasting, stunting, and concurrent wasting–stunting prevalence. The simulations were implemented in MATLAB using numerical ordinary differential equation solvers. In addition to model calibration analysis during the observation period, long-term projections were performed to evaluate the persistence and stabilization behavior of undernutrition dynamics up to the year 2050.

C. MATHEMATICAL FRAMEWORK

1. Model Assumptions

a. Population Structure

The under-five population is assumed to be homogeneous and well-mixed, without explicit spatial, socioeconomic, or behavioral stratification. This assumption is commonly adopted in compartmental modeling when only aggregated national-level data are available. The proposed framework focuses specifically on undernutrition interactions and therefore does not explicitly represent all possible nutritional categories within the population, such as overweight or obesity. Consequently, the modeled nutritional states should not be interpreted as a complete partition of the under-five population.

b. Nutritional State Transitions

Transitions between acute malnutrition states follow a progressive deterioration structure:

$$A \rightarrow B \rightarrow C,$$

representing the worsening of acute nutritional deficits from moderate to severe wasting. This assumption is supported by clinical and epidemiological evidence indicating that severe wasting generally develops progressively rather than instantaneously. Recovery is assumed to occur sequentially:

$$C \rightarrow B \rightarrow A,$$

reflecting staged nutritional rehabilitation processes commonly observed in child nutrition interventions.

c. Pathways to Stunting

Stunting is assumed to arise through multiple pathways:

$$A \rightarrow S, \quad B \rightarrow S, \quad C \rightarrow S.$$

This assumption reflects the multifactorial nature of chronic malnutrition. In addition to acute nutritional deficits, stunting may result from prolonged dietary inadequacy, recurrent infections, poor sanitation, environmental enteric dysfunction, and other long-term socioeconomic and environmental factors.

The direct pathway

$$A \rightarrow S$$

therefore represents chronic non-acute mechanisms contributing to impaired linear growth.

d. Irreversibility of Stunting

Individuals in the stunted compartment are assumed not to return to previous nutritional states:

$$S \nrightarrow A, B, C.$$

Biologically, recovery from stunting is not strictly zero; however, it is highly limited and occurs with very low probability, particularly after the first 1000 days of life. Empirical studies indicate that while partial catch-up growth may be observed, it is generally insufficient to fully reverse established linear growth deficits at the population level (De Onis & Branca, 2016; Mertens et al., 2023).

e. Age-Dependent Recovery

The model distinguishes between infants (<1 year), and non-infants (≥ 1 year). Infants are assumed to have higher recovery rates due to greater biological plasticity, higher responsiveness to nutritional interventions, critical growth windows in early life. This assumption is consistent with findings in child nutrition literature emphasizing the importance of early-life interventions (Mertens et al., 2023).

f. Mortality and Exit Processes

All compartments are assumed to experience identical mortality and exit rates ($\mu + \delta$). While mortality is known to differ by nutritional status, this simplification is adopted due to the lack of disaggregated mortality data and to maintain model tractability.

g. Data and Parameter Assumptions

The model is calibrated using aggregated annual data, implying that: (i) individual-level variability is not explicitly represented, (ii) parameters are assumed constant over each simulation period, (iii) the system is deterministic and does not account for stochastic fluctuations.

h. Representation of Interventions

Nutritional interventions, such as supplementary feeding programs (PMT), are incorporated implicitly through recovery parameters. Changes in these parameters represent improvements in intervention coverage, effectiveness, or access.

2. Model Formulation

We develop a deterministic compartmental model to describe the interaction between wasting and stunting dynamics among children under five years of age. The population is partitioned into four mutually exclusive nutritional states: $A(t)$ is number of well-nourished (normal) children, $B(t)$ is number of moderately wasted children, $C(t)$ is number of severely wasted children, and $S(t)$ is number of stunted children. The stunting compartment $S(t)$ represents the total proportion of children with impaired linear growth (height-for-age deficit), including those who simultaneously experience wasting. Thus, the model does not explicitly separate concurrent wasting–stunting cases; instead, these are implicitly included within the stunting compartment. The dynamics of the system are governed by:

$$\begin{aligned}
 \frac{dA}{dt} &= q_A \Lambda - (\gamma_{AB} + \gamma_{AS} + \mu + \delta)A + \phi_1^{eff} B, \\
 \frac{dB}{dt} &= q_B \Lambda + \gamma_{AB} A - (\phi_1^{eff} + \gamma_{BC} + \gamma_{BS} + \mu + \delta)B + \phi_2^{eff} C, \\
 \frac{dC}{dt} &= \gamma_{BC} B - (\phi_2^{eff} + \gamma_{CS} + \mu + \delta)C, \\
 \frac{dS}{dt} &= \gamma_{AS} A + \gamma_{BS} B + \gamma_{CS} C - (\mu + \delta)S.
 \end{aligned}
 \tag{1}$$

Each equation in system (1) represents the balance between inflow and outflow processes within the nutritional states. The compartment $A(t)$ increases through recruitment and recovery from moderate wasting, while decreasing due to progression toward wasting and stunting conditions. The compartment $B(t)$ acts as an intermediate acute malnutrition state, receiving individuals from nutritional deterioration and redistributing them through recovery, worsening nutritional status, and progression to stunting. The compartment $C(t)$ represents severe acute malnutrition, with transitions determined by worsening from moderate wasting and partial recovery processes. Meanwhile, the stunting compartment $S(t)$ represents chronic growth failure accumulated from all nutritional states and does not include an explicit recovery pathway, reflecting the long-term persistence of stunting conditions during early childhood.

To capture heterogeneity in recovery dynamics, the effective recovery rates are defined as:

$$\begin{aligned} \phi_i^{eff} &= \theta\phi_i^{inf} + (1 - \theta)\phi_i^{non}, \quad i = 1,2, \\ \theta &= \frac{N_{<1}}{N}, \end{aligned} \tag{2}$$

where: ϕ_i^{eff} is effective recovery rate type- i ; $N_{<1}$ is the number of infants aged below 1 year (0–11 months); ϕ_i^{inf} is recovery rate type- i for infants (<1 year); and ϕ_i^{non} is recovery rate type- i for children aged ≥ 1 year. This formulation reflects empirical findings that younger children exhibit higher physiological plasticity and faster recovery from wasting due to improved responsiveness to nutritional interventions during early life. The following is the explanation of the symbols used in the formula, which is summarized in Table 1.

Table 1. Description of symbols in the model

Symbol	Description	Unit
$A(t)$	Number of children in the well-nourished (normal) nutritional state at time t	individuals
$B(t)$	Number of children in the moderately wasted (moderate undernutrition) state at time t	individuals
$C(t)$	Number of children in the severely wasted (severe undernutrition) state at time t	individuals
$S(t)$	Number of children in the stunted (chronic malnutrition) state at time t	individuals
$N(t)$	Total number of children under five years old	individuals
$N_{<1}$	Number of infants aged below 1 year (0–11 months)	individuals
Λ	Total number of live births entering the population per unit time	Individuals. time ⁻¹
q_A	Proportion of newborns entering the well-nourished state	dimensionless
q_B	Proportion of newborns entering the wasting state (e.g., low birth weight)	dimensionless
γ_{AB}	Transition rate from well-nourished (A) to moderate wasting (B)	time ⁻¹
γ_{BC}	Transition rate from moderate wasting (B) to severe wasting (C)	time ⁻¹
γ_{AS}	Transition rate from well-nourished (A) directly to stunting (S) due to chronic factors	time ⁻¹
γ_{BS}	Transition rate from moderate wasting (B) to stunting (S)	time ⁻¹
γ_{CS}	Transition rate from severe wasting (C) to stunting (S)	time ⁻¹
ϕ_1^{eff}	Effective recovery rate from moderate wasting (B) to well-nourished (A)	time ⁻¹
ϕ_2^{eff}	Effective recovery rate from severe wasting (C) to moderate wasting (B)	time ⁻¹
ϕ_i^{inf}	Recovery rate for infants (<1 year), representing high recovery potential	time ⁻¹
ϕ_i^{non}	Recovery rate for children aged ≥ 1 year, representing lower recovery potential	time ⁻¹
θ	Proportion of infants (<1 year) in the population, used as a weighting factor in recovery rates	dimensionless
μ	Natural mortality rate of children	time ⁻¹
δ	Exit rate due to aging out of the under-five population	time ⁻¹

3. Nondimensionalization and Scaling

To simplify the analysis and reduce parameter redundancy, the model is transformed into a dimensionless form. This scaling procedure rescales both the state variables and time, allowing all transition parameters to be interpreted relative to a common baseline rate. Such an approach is widely used in dynamical systems modeling because it improves analytical tractability and facilitates comparisons across different populations and epidemiological settings. Since the model is calibrated using prevalence-based nutritional indicators, the state variables are represented in normalized form relative to the total under-five population. However, the modeled nutritional states do not constitute a complete partition of the population because stunting may overlap with wasting conditions, while other nutritional categories such as overweight or obesity are not explicitly incorporated into the framework. Define the normalized variables:

$$a = \frac{A}{N}, b = \frac{B}{N}, c = \frac{C}{N}, s = \frac{S}{N},$$

where N denotes the total under-five population. Under this formulation, $a(t)$, $b(t)$, $c(t)$, and $s(t)$ represent normalized prevalence-type nutritional indicators rather than mutually exclusive population fractions. Consequently, the total quantity

$$a(t) + b(t) + c(t) + s(t)$$

is not required to equal unity, since overlapping nutritional conditions may occur within the modeled population. In addition, the proposed framework focuses specifically on undernutrition interactions and does not explicitly include all nutritional categories, particularly overweight and obesity. Therefore, the modeled variables do not represent an exhaustive partition of the under-five population.

To eliminate dimensional dependence on time, we introduce the dimensionless timescale:

$$\tau = (\mu + \delta)t.$$

Applying the chain rule gives:

$$\frac{d}{dt} = (\mu + \delta) \frac{d}{d\tau}.$$

This scaling normalizes all transition rates relative to the baseline removal rate $(\mu + \delta)$. Define the following dimensionless parameters:

$$\begin{aligned} \beta_1 &= \frac{\gamma_{AB}}{\mu + \delta}, & \beta_2 &= \frac{\gamma_{BC}}{\mu + \delta}, \\ \eta_1 &= \frac{\gamma_{AS}}{\mu + \delta}, & \eta_2 &= \frac{\gamma_{BS}}{\mu + \delta}, & \eta_3 &= \frac{\gamma_{CS}}{\mu + \delta}, \\ \rho_1 &= \frac{\phi_1^{eff}}{\mu + \delta}, & \rho_2 &= \frac{\phi_2^{eff}}{\mu + \delta}. \end{aligned}$$

Substituting these transformations into the original system yields:

$$\begin{aligned}
 \frac{da}{d\tau} &= q_A \tilde{\Lambda} - (\beta_1 + \eta_1 + 1)a + \rho_1 b, \\
 \frac{db}{d\tau} &= q_B \tilde{\Lambda} + \beta_1 a - (\rho_1 + \beta_2 + \eta_2 + 1)b + \rho_2 c \\
 \frac{dc}{d\tau} &= \beta_2 b - (\rho_2 + \eta_3 + 1)c, \\
 \frac{ds}{d\tau} &= \eta_1 a + \eta_2 b + \eta_3 c - s,
 \end{aligned} \tag{3}$$

where $\tilde{\Lambda} = \frac{\Lambda}{N(\mu+\delta)}$ denotes the dimensionless recruitment rate. System (3) therefore represents the standardized dimensionless model in which:

- i. all transition parameters are expressed relative to the baseline removal rate $(\mu+\delta)$,
- ii. the constant term “1” corresponds to the normalized effect of mortality and aging,
- iii. the system becomes independent of absolute population scale,
- iv. the state variables represent normalized prevalence-type nutritional indicators rather than mutually exclusive population fractions.

For example, $\beta_1 + \eta_1 + 1$ represents the total normalized rate at which individuals leave the a -class due to progression toward wasting, transition to stunting, and removal through mortality and aging processes.

4. Positivity and Boundedness of Solutions

In this section, we establish the fundamental qualitative properties of the system (3), including positivity, boundedness, and well-posedness. These properties ensure that the model remains biologically meaningful and mathematically consistent.

Lemma 1 (Positivity of Solutions)

Assume that all parameters $q_A, q_B, \beta_1, \beta_2, \eta_1, \eta_2, \eta_3, \rho_1, \rho_2$ are nonnegative and the initial condition satisfies $a(0), b(0), c(0), s(0) \geq 0$. Then, for all $\tau \geq 0$, $a(\tau), b(\tau), c(\tau), s(\tau) \geq 0$.

Proof.

Let $x(\tau) = (a, b, c, s)^T \in \mathbb{R}_{\geq 0}^4$. The system (3) can be written as $\dot{x} = F(x)$, where F is continuously differentiable and affine in x , hence locally Lipschitz. By the Picard–Lindelöf theorem, a unique solution exists. To prove positivity, we evaluate the vector field on the boundary:

For $a = 0$:

$$\frac{da}{d\tau} = q_A + \rho_1 b \geq 0.$$

For $b = 0$:

$$\frac{db}{d\tau} = q_B + \beta_1 a + \rho_2 c \geq 0.$$

For $c = 0$:

$$\frac{dc}{d\tau} = \beta_2 b \geq 0.$$

For $s = 0$:

$$\frac{ds}{d\tau} = \eta_1 a + \eta_2 b + \eta_3 c \geq 0.$$

Thus, trajectories cannot leave the nonnegative orthant. Therefore,

$$a(\tau), b(\tau), c(\tau), s(\tau) \geq 0, \forall \tau \geq 0. \quad \square \tag{4}$$

This result guarantees that all state variables, interpreted as population proportions, remain nonnegative over time, ensuring biological feasibility.

Lemma 2 (Invariant Region and Boundedness)

Consider the nonnegative region $\Omega = \{(a, b, c, s) \in \mathbb{R}_{\geq 0}^4 : a + b + c + s \leq M\}$, for some positive constant $M > 0$. Then, the region Ω is positively invariant under system (3).

Proof

Let $T(\tau) = a(\tau) + b(\tau) + c(\tau) + s(\tau)$. Summing all equations in system (3) yields

$$\frac{dT}{d\tau} = q_A + q_B - T.$$

Since $q_A + q_B = 1$, we obtain

$$\frac{dT}{d\tau} = 1 - T.$$

The corresponding solution is

$$T(\tau) = 1 + (T(0) - 1)e^{-\tau}.$$

Hence, $\lim_{\tau \rightarrow \infty} T(\tau) = 1$. Moreover, if $T(0) \leq M$, then

$$T(\tau) \leq \max\{T(0), 1\} \leq M, \forall \tau \geq 0.$$

Therefore, trajectories remain inside the region Ω , implying that Ω is positively invariant. \square

Lemma 3 (Global Boundedness)

All solutions of system (3) remain nonnegative and bounded for all $\tau \geq 0$.

Proof

From Lemma 1, $a(\tau), b(\tau), c(\tau), s(\tau) \geq 0, \forall \tau \geq 0$. Furthermore, Lemma 2 implies that $T(\tau) = a(\tau) + b(\tau) + c(\tau) + s(\tau)$ remains bounded for all time. Since each variable is nonnegative, we obtain $0 \leq a(\tau), b(\tau), c(\tau), s(\tau) \leq T(\tau), \forall \tau \geq 0$. Because $T(\tau)$ is bounded, each state variable is also bounded. Therefore, all solutions remain inside a compact positively invariant region of $\mathbb{R}_{\geq 0}^4$. \square

This result guarantees that the proposed model remains mathematically well-posed and biologically feasible over time. In particular, the state variables cannot become negative or diverge to unbounded values, ensuring that the long-term dynamics remain epidemiologically meaningful and suitable for equilibrium and stability analysis.

5. Model's Steady State

A steady state (equilibrium point) of system (3) is defined as a constant vector $E^* = (a^*, b^*, c^*, s^*)$, for which all state variables remain constant over time. The equilibrium is obtained by setting $\frac{da}{d\tau} = \frac{db}{d\tau} = \frac{dc}{d\tau} = \frac{ds}{d\tau} = 0$, thereby transforming the dynamical system into a set of algebraic balance equations. Any biologically admissible equilibrium must satisfy $a^*, b^*, c^*, s^* \geq 0$. To simplify the equilibrium analysis, define the following composite parameters:

$$\begin{aligned} k_A &= \beta_1 + \eta_1 + 1, \\ k_B &= \rho_1 + \beta_2 + \eta_2 + 1, \\ k_C &= \rho_2 + \eta_3 + 1 \end{aligned} \tag{7}$$

Substituting the equilibrium conditions (7) into system (3) yields

$$\begin{aligned} q_A - k_A a^* + \rho_1 b^* &= 0, \\ q_B + \beta_1 a^* - k_B b^* + \rho_2 c^* &= 0, \\ \beta_2 b^* - k_C c^* &= 0, \\ \eta_1 a^* + \eta_2 b^* + \eta_3 c^* - s^* &= 0 \end{aligned} \tag{8}$$

From the third equation of (8), the equilibrium value of c^* can be expressed in terms of b^* as

$$c^* = \frac{\beta_2}{k_C} b^*. \tag{9}$$

Substituting (9) into the second equation of (8) gives

$$q_B + \beta_1 a^* - \left(k_B - \frac{\rho_2 \beta_2}{k_C} \right) b^* = 0. \tag{10}$$

Define the effective parameter

$$\tilde{k}_B = k_B - \frac{\rho_2 \beta_2}{k_C}. \tag{11}$$

Hence,

$$b^* = \frac{q_B + \beta_1 a^*}{\tilde{k}_B}. \tag{12}$$

Substituting (12) into the first equation of (8) yields

$$q_A - k_A a^* + \rho_1 \frac{q_B + \beta_1 a^*}{\tilde{k}_B} = 0.$$

Rearranging terms, we obtain

$$a^* = \frac{q_A + \frac{\rho_1}{\tilde{k}_B} q_B}{k_A - \frac{\rho_1 \beta_1}{\tilde{k}_B}}. \tag{13}$$

Using equations (9), (12), and (13), all equilibrium components can be written recursively as

$$\begin{aligned} a^* &= \frac{q_A + \frac{\rho_1}{\tilde{k}_B} q_B}{k_A - \frac{\rho_1 \beta_1}{\tilde{k}_B}}, \\ b^* &= \frac{q_B + \beta_1 a^*}{\tilde{k}_B}, \\ c^* &= \frac{\beta_2}{k_C} b^*, \\ s^* &= \eta_1 a^* + \eta_2 b^* + \eta_3 c^*. \end{aligned} \tag{14}$$

The equilibrium solution remains biologically admissible provided that $k_C > 0$, $\tilde{k}_B > 0$, and $k_A - \frac{\rho_1 \beta_1}{\tilde{k}_B} > 0$. These conditions ensure that all denominators remain positive and the equilibrium is well-defined and nonnegative. The equilibrium analysis demonstrates that the long-term nutritional dynamics are governed by a cascade of deterioration and recovery processes originating from wasting progression pathways. The recursive structure of the equilibrium solution also provides a biologically interpretable representation of how deterioration rates, recovery mechanisms, and progression toward stunting collectively determine the long-term undernutrition burden within the population.

6. Threshold Analysis of Wasting Dynamics

To characterize the persistence or decay of wasting dynamics, we derive a threshold quantity analogous to the basic reproduction number in epidemiological models. We focus on the subsystem governing moderate and severe wasting:

$$\begin{aligned} \frac{db}{d\tau} &= \beta_1 a - k_B b + \rho_2 c, \\ \frac{dc}{d\tau} &= \beta_2 b - k_C c, \end{aligned} \tag{15}$$

To analyze the initial wasting dynamics, we linearize the subsystem around a low-wasting regime where $(b, c) \approx (0, 0)$, while the normalized prevalence variable a remains approximately constant. The linearized system becomes

$$\begin{pmatrix} \dot{b} \\ \dot{c} \end{pmatrix} = \begin{pmatrix} -k_B & \rho_2 \\ \beta_2 & -k_C \end{pmatrix} \begin{pmatrix} b \\ c \end{pmatrix} + \begin{pmatrix} \beta_1 a \\ 0 \end{pmatrix}.$$

Using a matrix decomposition approach analogous to the next-generation framework, define

$$F = \begin{pmatrix} \beta_1 & 0 \\ 0 & 0 \end{pmatrix}, V = \begin{pmatrix} k_B & -\rho_2 \\ -\beta_2 & k_C \end{pmatrix}.$$

The threshold quantity is defined as $\mathcal{R}_W = \rho(FV^{-1})$, where $\rho(\cdot)$ denotes the spectral radius. Straightforward computation yields

$$\mathcal{R}_W = \frac{\beta_1 k_C}{k_B k_C - \rho_2 \beta_2}. \tag{16}$$

The threshold quantity \mathcal{R}_W characterizes the relative balance between deterioration into wasting states and the combined recovery/removal mechanisms within the wasting subsystem. Specifically, the numerator $\beta_1 k_C$ captures the effective deterioration pressure toward wasting, while the denominator $k_B k_C - \rho_2 \beta_2$ represents the combined stabilization effect generated by recovery, removal, and internal feedback between moderate and severe wasting compartments. Consequently, if $\mathcal{R}_W < 1$, recovery and removal mechanisms dominate, causing wasting dynamics to decay over time; whereas $\mathcal{R}_W > 1$ indicates that deterioration mechanisms dominate, allowing wasting dynamics to persist within the population.

7. Local Stability Analysis

Theorem 1

Let $E^* = (a^*, b^*, c^*, s^*)$ be a biologically feasible equilibrium point of system (3). Under biologically admissible positive parameters, the equilibrium E^* is locally asymptotically stable when $\mathcal{R}_W < 1$.

Proof

The local stability of E^* is determined by the eigenvalues of the Jacobian matrix associated with the wasting subsystem:

$$J_{ABC} = \begin{pmatrix} -k_A & \rho_1 & 0 \\ \beta_1 & -k_B & \rho_2 \\ 0 & \beta_2 & -k_C \end{pmatrix},$$

The characteristic polynomial of J_{ABC} is

$$\lambda^3 + a_1 \lambda^2 + a_2 \lambda + a_3 = 0, \tag{17}$$

where

$$a_1 = k_A + k_B + k_C,$$

$$a_2 = k_A k_B + k_A k_C + k_B k_C - \rho_1 \beta_1 - \rho_2 \beta_2, \tag{18}$$

$$a_3 = k_A (k_B k_C - \rho_2 \beta_2) - \rho_1 \beta_1 k_C.$$

According to the Routh–Hurwitz criterion, the equilibrium point is locally asymptotically stable if

$$a_1 > 0, \quad a_2 > 0, \quad a_3 > 0, \quad a_1 a_2 > a_3. \tag{19}$$

Since all parameters are assumed positive, we immediately obtain $a_1 > 0$. From the definition of the threshold quantity in equation (16), when $\mathcal{R}_W < 1$ implies

$$\beta_1 k_C < k_B k_C - \rho_2 \beta_2.$$

Rearranging yields

$$k_B k_C > \rho_2 \beta_2 + \beta_1 k_C > \rho_2 \beta_2. \tag{20}$$

Consequently,

$$k_B k_C - \rho_2 \beta_2 > 0. \tag{21}$$

Biologically, this condition implies that the combined recovery and removal mechanisms within the wasting subsystem dominate the internal deterioration feedback between moderate and severe wasting states. Therefore, wasting amplification remains controlled rather than self-reinforcing. Using inequality (20), we examine the coefficient

$$a_2 = k_A k_B + k_A k_C + k_B k_C - \rho_1 \beta_1 - \rho_2 \beta_2.$$

since $k_B k_C > \rho_2 \beta_2$, we obtain

$$a_2 > k_A k_B + k_A k_C - \rho_1 \beta_1.$$

Because

$$k_A = \beta_1 + \eta_1 + 1, \quad k_B = \rho_1 + \beta_2 + \eta_2 + 1,$$

all remaining terms in the expansion of $k_A k_B$ are positive, implying

$$k_A k_B > \rho_1 \beta_1. \tag{22}$$

Hence, $a_2 > 0$.

Similarly, for

$$a_3 = k_A(k_B k_C - \rho_2 \beta_2) - \rho_1 \beta_1 k_C.$$

Since $\beta_1 k_C < k_B k_C - \rho_2 \beta_2$ (inequality (20)), we obtain

$$\rho_1 \beta_1 k_C < \rho_1(k_B k_C - \rho_2 \beta_2).$$

Therefore,

$$a_3 > (k_A - \rho_1)(k_B k_C - \rho_2 \beta_2).$$

Since all parameters are positive and

$$k_B k_C - \rho_2 \beta_2 > 0, \tag{23}$$

it follows that

$$a_3 > 0.$$

Now, we compute

$$a_1 a_2 - a_3.$$

Substituting the expressions for a_1, a_2, a_3 in equation (18) yields

$$a_1 a_2 - a_3 = (k_A + k_B + k_C)(k_A k_B + k_A k_C + k_B k_C - \rho_1 \beta_1 - \rho_2 \beta_2) - [k_A(k_B k_C - \rho_2 \beta_2) - \rho_1 \beta_1 k_C].$$

Expanding and rearranging terms gives

$$a_1 a_2 - a_3 = k_A^2 k_B + k_A^2 k_C + k_A k_B^2 + k_A k_C^2 + k_B^2 k_C + k_B k_C^2 + 2k_A k_B k_C - k_A \rho_1 \beta_1 - k_B \rho_1 \beta_1 - k_A \rho_2 \beta_2 - k_C \rho_2 \beta_2 + \rho_1 \beta_1 k_C. \tag{24}$$

All cubic and quadratic terms involving k_A, k_B, k_C are strictly positive. Moreover, from condition $k_B k_C > \rho_2 \beta_2$ (equation (23)), together with $\beta_1 k_C < k_B k_C - \rho_2 \beta_2$ (inequality 20), the negative terms remain dominated by the positive stabilizing contributions associated with the recovery and removal structure. Since all parameters are positive and the stabilizing terms dominate the deterioration feedback terms, it follows that

$$a_1 a_2 - a_3 > 0. \tag{25}$$

Therefore, all Routh–Hurwitz conditions are satisfied:

$$a_1 > 0, a_2 > 0, a_3 > 0, a_1 a_2 > a_3.$$

Consequently, all eigenvalues of the Jacobian matrix possess negative real parts, implying that the equilibrium point E^* is locally asymptotically stable whenever $\mathcal{R}_W < 1$. The threshold quantity \mathcal{R}_W therefore serves as a key indicator governing both wasting persistence and local stability behavior of the system. In particular:

- i. $\mathcal{R}_W < 1$ implies decay of wasting dynamics and convergence toward equilibrium,
- ii. whereas $\mathcal{R}_W > 1$ indicates persistence of wasting and the potential emergence of a higher endemic undernutrition equilibrium.

From a biological perspective, the condition $\mathcal{R}_W < 1$ may be achieved by: (i) increasing recovery rates (ρ_1, ρ_2), (ii) reducing deterioration rates (β_1, β_2), and (iii) lowering progression toward stunting (η_1, η_2, η_3). These findings support integrated nutritional interventions emphasizing early wasting prevention, recovery improvement, maternal nutrition enhancement, sanitation, infection prevention, and long-term child nutritional monitoring.

D. RESULT AND DISCUSSION

1. Calibration and Estimation Parameters

The model parameters were estimated by fitting the dimensional form of the system to observed prevalence data of moderate wasting, severe wasting, and stunting. The calibration was performed using a nonlinear least squares approach. Let $Y_{\text{data}}(t) = (b_{\text{data}}(t), c_{\text{data}}(t), s_{\text{data}}(t))$ denote the observed data, and $Y_{\text{model}}(t; \theta)$ the corresponding model outputs. The parameter vector θ was estimated by minimizing the objective function:

$$\min_{\theta} \sum_t [(b(t) - b_{\text{data}}(t))^2 + (c(t) - c_{\text{data}}(t))^2 + (s(t) - s_{\text{data}}(t))^2], \tag{26}$$

augmented with a penalty term to enforce biologically consistent ordering of transition rates:

$$\eta_1 \leq \eta_2 \leq \eta_3. \tag{27}$$

The optimization was implemented using the Levenberg–Marquardt algorithm via MATLAB’s `lsqnonlin` function. To incorporate age-dependent recovery, the recovery parameters were modeled as convex combinations weighted by the proportion of infants. Additionally, the concurrent wasting–stunting prevalence was incorporated indirectly as a derived quantity:

$$D(t) = \kappa S(t), \tag{28}$$

where κ is determined from baseline data (2013).

The calibration procedure utilized aggregated demographic and nutritional prevalence data collected from national reports in Indonesia during 2013–2024. Data for 2020–2021 were not included in the calibration process because nutritional surveillance and reporting activities during the COVID-19 pandemic period were substantially disrupted, potentially affecting data consistency and comparability across years. The dataset includes under-five population size, infant population, live birth statistics, and prevalence indicators for wasting, severe wasting, and stunting. These variables were used to construct demographic trajectories and prevalence targets for the calibration process. Prior to parameter estimation, preprocessing procedures were performed to ensure temporal consistency and biological plausibility of the dataset, including interpolation-based reconstruction of incomplete demographic observations and correction of anomalous infant population data. The integrated demographic and prevalence data used for model calibration are summarized in Table 2.

Table 2. Integrated Demographic and Prevalence Data used for Calibration

Year	Under-Five Population	Infants (0 yr)	Live Births	LBW	Wasting	Severe Wasting	Stunting
2013	23,700,676	4,396,537	4,735,692	0.102	0.068	0.053	0.376
2016	23,960,110	4,770,444	4,867,813	NA	0.0887	0.0368	0.1463
2017	23,848,283	4,764,638	4,840,511	NA	0.067	0.028	0.296
2018	23,729,583	4,720,024	4,810,130	0.040	0.067	0.035	0.308

Year	Under-Five Population	Infants (0 yr)	Live Births	LBW	Wasting	Severe Wasting	Stunting
2022	21,856,192	4,373,429	4,452,717	0.033	0.067	0.010	0.216
2023	22,511,838	4,495,989*	4,030,995	0.039	0.077	0.008	0.215
2024	22,638,079	4,618,549	4,591,129	0.037			

*The original infant population value reported for 2023 was excluded from the analysis because it exhibited substantial inconsistency relative to the surrounding demographic observations. Therefore, the 2023 infant population was approximated using linear interpolation between the 2022 and 2024 demographic values to maintain temporal consistency in the age-dependent recovery calculations

Using the demographic and prevalence data summarized in Table 2, the nonlinear least-squares optimization procedure was performed to estimate the unknown transition and recovery parameters of the model. The calibration process produced a final residual value of 0.00877, indicating good agreement between simulated trajectories and observed prevalence data. The resulting parameter set used in subsequent simulations and analyses is summarized in Table 3. Table 3 shows that the deterioration rate from the well-nourished state toward moderate wasting, β_1 , remains relatively small, whereas the progression rate from moderate wasting to severe wasting, β_2 , is substantially larger. This indicates that acute malnutrition generally develops gradually under stable population conditions, but nutritional deterioration may accelerate considerably once moderate wasting occurs.

Table 3. Parameter Values used for Calibration and Simulation.

Symbol	Value	Unit	Method	Source
β_1	0.0113	year ⁻¹	Estimated by least-squares calibration	Indonesian prevalence data (2013–2024)
β_2	0.1273	year ⁻¹	Estimated by least-squares calibration	Indonesian prevalence data (2013–2024)
η_1	0.0035	year ⁻¹	Estimated by least-squares calibration	Indonesian prevalence data (2013–2024)
η_2	0.3433	year ⁻¹	Estimated by least-squares calibration	Indonesian prevalence data (2013–2024)
η_3	0.3434	year ⁻¹	Estimated by least-squares calibration	Indonesian prevalence data (2013–2024)
ρ_1^{inf}	0.4851	year ⁻¹	Estimated by least-squares calibration	Indonesian prevalence data (2013–2024)
ρ_1^{non}	0.4381	year ⁻¹	Estimated by least-squares calibration	Indonesian prevalence data (2013–2024)
ρ_2^{inf}	0.0877	year ⁻¹	Estimated by least-squares calibration	Indonesian prevalence data (2013–2024)
ρ_2^{non}	0.0373	year ⁻¹	Estimated by least-squares calibration	Indonesian prevalence data (2013–2024)
q_A	0.96	–	Assumed/fixed	Baseline normalization assumption
q_B	0.04	–	Assumed/fixed	Based on baseline wasting prevalence
$\theta(t)$	Time-dependent	–	Computed from demographic data	Indonesian demographic statistics

The estimated direct transition rate from the well-nourished state toward stunting, η_1 , is comparatively low, suggesting that chronic growth failure among non-wasted children develops slowly through cumulative long-term mechanisms such as recurrent infection, poor dietary quality, maternal malnutrition, and socioeconomic deprivation. In contrast, the progression rates from moderate and severe wasting toward stunting, η_2 and η_3 , are relatively large and nearly identical, indicating that wasting substantially increases the risk of chronic growth impairment regardless of severity level. This finding supports the hypothesis that wasting and stunting are strongly interconnected forms of undernutrition.

The estimated recovery parameters further indicate that the recovery rates from moderate wasting for infants and older children, ρ_1^{inf} and ρ_1^{non} , are relatively high, with infants recovering faster than older children. This supports the biological assumption underlying the proposed age-dependent recovery mechanism. However, the recovery rates from severe wasting, ρ_2^{inf} and ρ_2^{non} , remain substantially lower for both age groups, suggesting that severe acute malnutrition is considerably more difficult to reverse through nutritional rehabilitation alone. These results imply that preventing progression toward severe wasting may be substantially more effective than relying solely on treatment after severe deterioration has occurred.

Figure 2 presents the calibration results of the dimensional wasting–stunting model against observed prevalence data during 2013–2024. Overall, the simulated trajectories reproduce the dominant long-term dynamics of moderate wasting, severe wasting, and stunting with satisfactory agreement between numerical simulations and empirical observations. Moderate wasting exhibits relatively persistent behavior with gradual stabilization, whereas severe wasting shows a more pronounced decline over time. In contrast, stunting decreases more slowly and remains persistent throughout the observation period, reflecting the cumulative and multifactorial nature of chronic undernutrition dynamics.

The smoother simulated trajectories relative to empirical observations are expected because the proposed framework is deterministic and does not explicitly incorporate temporary disturbances such as seasonal food insecurity, infectious disease outbreaks, economic shocks, or variations in intervention coverage. Overall, the calibration results demonstrate that the proposed model provides a biologically plausible representation of both acute and chronic undernutrition dynamics while maintaining good consistency with observed prevalence data.

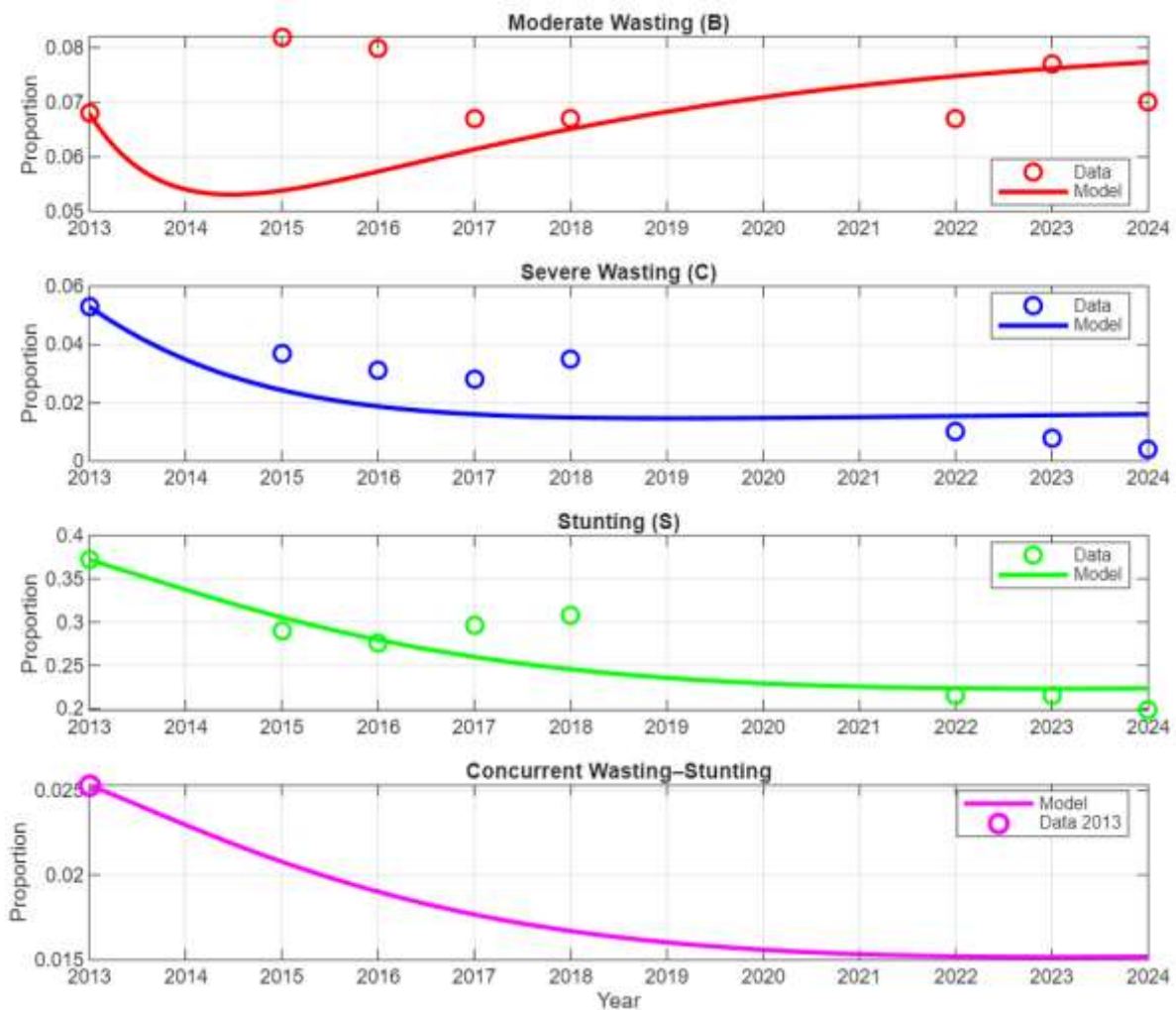


Figure 2. Calibration results of wasting-stunting dynamics model (2013-2024)

2. Sensitivity Analysis

To identify the most influential parameters governing the system dynamics, a local sensitivity analysis was performed using the normalized forward sensitivity index. For a given parameter p , the sensitivity index is defined as:

$$S_p = \frac{\partial S}{\partial p} \cdot \frac{p}{S}, \tag{25}$$

where S denotes the long-term stunting prevalence evaluated at the final simulation time. Each parameter was perturbed individually by a relative change of 10% while all remaining parameters were held constant. The resulting variation in the model output was then used to approximate the sensitivity indices numerically. The computed sensitivity indices are presented in Table 4 and Figure 3.

Table 4 presents the normalized local sensitivity indices of the nondimensional model parameters with respect to the long-term stunting prevalence. The sensitivity indices quantify the relative influence of each parameter on the system dynamics. Positive sensitivity values indicate that increasing the corresponding parameter increases long-term stunting prevalence,

whereas negative values indicate parameters that reduce chronic undernutrition prevalence when increased.

Table 4. Normalized Sensitivity Indices of the Nondimensional Model Parameters

Rank	Parameter	Sensitivity Index	Interpretation
1	β_1	0.3613	Transition from the normal nutritional state to moderate wasting is the most influential driver increasing long-term stunting prevalence.
2	η_2	0.3445	Progression from moderate wasting toward stunting strongly contributes to chronic undernutrition persistence.
3	η_1	0.3062	Direct progression from the normal nutritional state to stunting substantially influences chronic growth failure dynamics.
4	ρ_1^{non}	-0.1943	Improved recovery from moderate wasting among non-infants reduces long-term stunting prevalence.
5	ρ_1^{inf}	-0.0653	Faster infant recovery from moderate wasting contributes to reductions in chronic undernutrition.
6	η_3	0.0473	Severe wasting progression toward stunting contributes positively but with relatively smaller influence.
7	β_2	0.0455	Transition from moderate wasting to severe wasting has limited but positive influence on stunting prevalence.
8	ρ_2^{non}	-0.0024	Recovery from severe wasting among non-infants exhibits minimal long-term influence under the current model configuration.
9	ρ_2^{inf}	-0.0017	Infant recovery from severe wasting shows negligible sensitivity influence on the long-term stunting equilibrium.

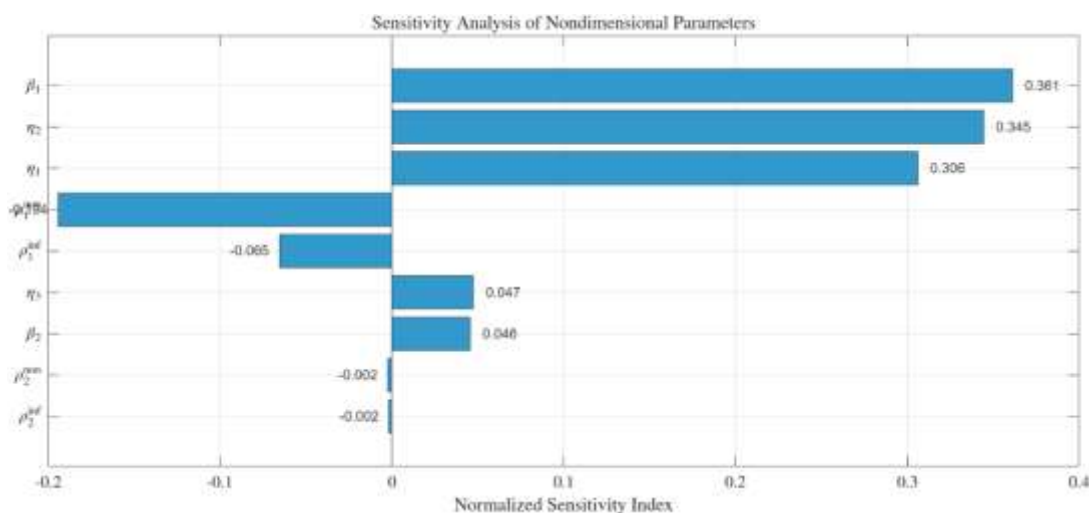


Figure 3. Sensitivity analysis of nondimensional parameters

The results demonstrate that the parameter β_1 has the largest positive sensitivity index, $S_{\beta_1} = 0.3613$. This parameter represents the transition from the normal nutritional state toward moderate wasting. Its dominant sensitivity value indicates that early deterioration into wasting is the most influential mechanism governing long-term stunting dynamics within the proposed system. Epidemiologically, this finding suggests that preventing the onset of wasting may produce substantial long-term reductions in chronic undernutrition prevalence. The result

is consistent with previous nutritional studies showing that wasting episodes during childhood substantially increase the risk of subsequent growth failure through impaired nutrient utilization, recurrent infection, and inflammatory stress. From a public health perspective, this finding emphasizes the importance of preventive interventions such as food security improvement, breastfeeding promotion, dietary adequacy, and early nutritional surveillance programs.

The second and third most influential parameters are: $\eta_2 = 0.3445$, $\eta_1 = 0.3062$. These parameters describe progression toward stunting from moderate wasting and from the normal nutritional state, respectively. Their large positive sensitivity values indicate that chronic growth failure is driven not only by acute wasting pathways but also by broader long-term nutritional and environmental determinants. In particular, the large value of η_2 reinforces the strong epidemiological linkage between wasting and stunting identified during model calibration. This finding supports the hypothesis that wasting and stunting represent interconnected manifestations of undernutrition rather than biologically independent conditions. Meanwhile, the substantial sensitivity associated with η_1 suggests that stunting may also develop independently of wasting through chronic mechanisms such as maternal undernutrition, poor sanitation, recurrent infection, inadequate dietary diversity, and socioeconomic deprivation. This result aligns with the multifactorial conceptual framework of stunting proposed in global nutrition literature and implies that reducing wasting prevalence alone may not fully eliminate chronic growth failure at the population level.

The recovery parameters associated with moderate wasting exhibit negative sensitivity indices: $\rho_1^{\text{non}} = -0.1943$, $\rho_1^{\text{inf}} = -0.0653$. These negative values indicate that improving recovery from moderate wasting contributes to reductions in long-term stunting prevalence. Interestingly, the magnitude of $|\rho_1^{\text{non}}| > |\rho_1^{\text{inf}}|$ suggests that improving recovery among non-infant children may exert greater influence on population-level stunting reduction. One possible explanation is that non-infant children constitute a larger proportion of the under-five population and therefore contribute more strongly to the aggregate system dynamics. Nevertheless, both parameters highlight the importance of early nutritional rehabilitation and community-based wasting treatment programs in reducing long-term chronic undernutrition burden.

The parameters η_3 and β_2 show relatively smaller positive sensitivity values: $S_{\eta_3} = 0.0473$, $S_{\beta_2} = 0.0455$. Although severe wasting contributes positively to chronic undernutrition progression, its influence on long-term stunting prevalence appears substantially weaker than the moderate wasting pathway. This behavior may reflect the comparatively lower prevalence of severe wasting within the population, causing moderate wasting dynamics to dominate the long-term epidemiological behavior of the system. Biologically, moderate wasting may also persist for longer durations within the community, thereby exerting broader cumulative effects on growth impairment at the population level.

Finally, the recovery parameters associated with severe wasting, ρ_2^{non} and ρ_2^{inf} , exhibit sensitivity indices very close to zero: -0.0024 and -0.0017 , respectively. These near-zero values suggest that severe wasting recovery dynamics exert relatively limited structural influence on the long-term stunting equilibrium under the current model configuration. From a methodological perspective, such small sensitivity values may also indicate weaker

parameter identifiability caused by the relatively low prevalence of severe wasting and the limited temporal resolution of the aggregated national dataset. Importantly, these results do not imply that severe wasting treatment lacks clinical significance. Rather, they indicate that, at the population level, long-term stunting dynamics are more strongly influenced by early wasting prevention and moderate wasting recovery processes than by severe wasting recovery alone.

Overall, the sensitivity analysis reveals that the dominant drivers of chronic undernutrition dynamics are the initiation of wasting, progression from wasting toward stunting, and recovery from moderate wasting. These findings carry important implications for stunting management policies. In particular, the results suggest that intervention strategies focusing solely on severe wasting treatment may have limited long-term impact on population-level stunting prevalence. Instead, integrated interventions emphasizing early wasting prevention, timely treatment of moderate wasting, maternal nutrition improvement, sanitation enhancement, infection prevention, food security, and community-based nutritional monitoring are likely to produce more sustainable reductions in chronic undernutrition burden.

3. Projection Simulation

Figure 4 presents the long-term projection of childhood wasting–stunting dynamics from 2024 to 2050 using the calibrated dimensional model. Overall, the numerical simulations indicate that the undernutrition system evolves toward a dynamically stable low-endemic equilibrium characterized by substantial reductions in wasting and stunting prevalence together with a dominant increase in the well-nourished population. All trajectories remain biologically feasible throughout the simulation horizon and converge smoothly toward stable equilibrium levels, indicating stable long-term system behavior under the estimated parameter regime.

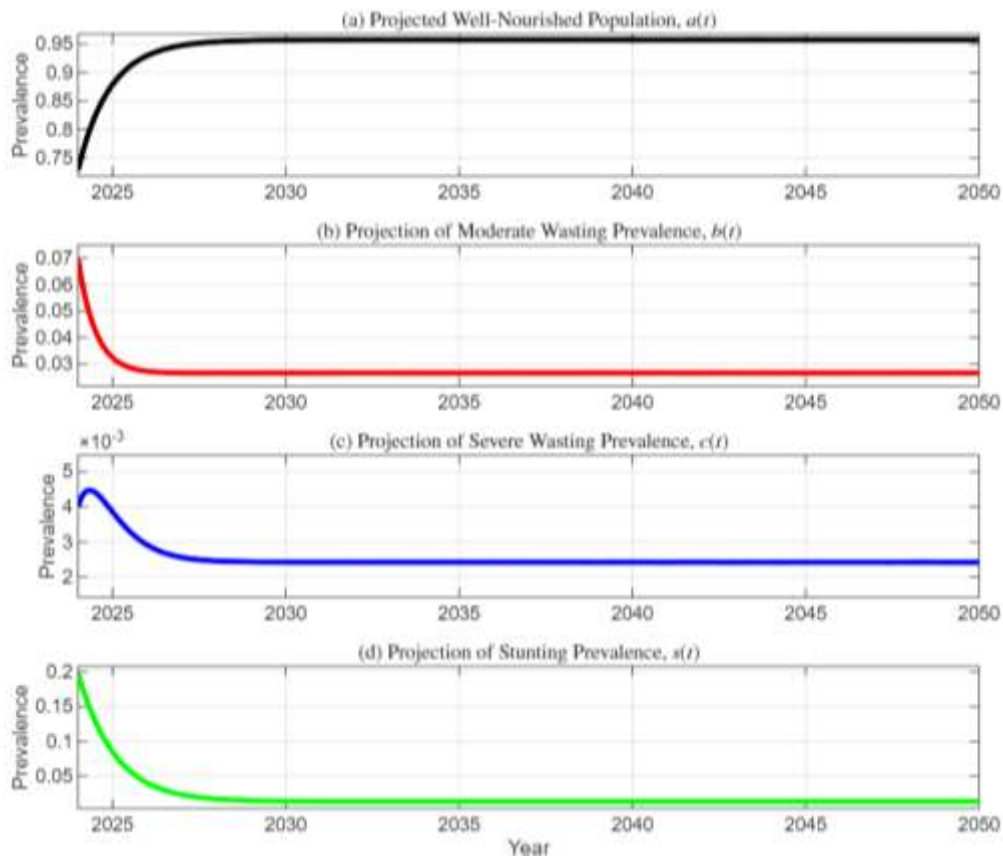


Figure 4. Long-term projection of childhood wasting–stunting dynamics from 2024 to 2050: (a) well-nourished population $a(t)$, (b) moderate wasting prevalence $b(t)$, (c) severe wasting prevalence $c(t)$, and (d) stunting prevalence $s(t)$

Figure 4(a) shows that the proportion of well-nourished children $a(t)$ increases rapidly during the early years of the projection period before gradually approaching a stable equilibrium close to unity. This behavior indicates that recovery-related mechanisms dominate nutritional deterioration pathways over the long term, allowing the healthy population compartment to become increasingly dominant within the system. Mathematically, the convergence of the well-nourished compartment toward a bounded positive equilibrium further confirms the positivity and boundedness properties established analytically. Epidemiologically, this result suggests that sustained nutritional recovery interventions, improvements in healthcare access, and reductions in severe nutritional deterioration may substantially increase the proportion of nutritionally healthy children over time.

In contrast, Figures 4(b) and Figures 4(c) demonstrate substantial reductions in both moderate wasting $b(t)$ and severe wasting $c(t)$ prevalence throughout the projection horizon. Moderate wasting declines sharply during the initial years before stabilizing at a low but strictly positive endemic level, whereas severe wasting decreases even more rapidly toward values approaching zero. The steeper decline observed in severe wasting suggests that severe acute malnutrition is highly responsive to recovery-related mechanisms within the calibrated parameter regime. Nevertheless, neither wasting compartment is completely eliminated, indicating that residual nutritional vulnerability continues to persist within the population despite substantial long-term improvements in nutritional conditions.

Figure 4(d) further illustrates that stunting prevalence $s(t)$ also decreases considerably over time. The trajectory initially declines rapidly before gradually approaching a low positive equilibrium level. Although stunting is generally more persistent than wasting because of its chronic and cumulative nature, the model predicts that long-term reductions in wasting prevalence combined with sustained recovery mechanisms gradually suppress chronic undernutrition as well. However, the persistence of positive stunting prevalence indicates that structural determinants of chronic malnutrition remain active within the population. Biologically and epidemiologically, this persistence reflects the multifactorial nature of stunting, which is influenced not only by wasting progression dynamics but also by maternal nutrition, household food insecurity, sanitation quality, recurrent infections, poverty, and broader environmental conditions.

Importantly, the numerical projections strongly support the analytical results associated with the wasting threshold \mathcal{R}_W . Since the estimated value of \mathcal{R}_W remains consistently below unity throughout the projection horizon, the deterioration pathways driving wasting progression are substantially weaker than the combined recovery and removal mechanisms operating within the system. Consequently, the wasting dynamics cannot sustain long-term endemic amplification, causing all prevalence trajectories to progressively decline and converge toward stable equilibrium states. The smooth convergence observed in all state variables therefore provides strong numerical validation of the theoretical local stability analysis established previously.

The simulation results also demonstrate the epidemiological significance of the threshold condition $\mathcal{R}_W < 1$. In the context of the present model, this threshold implies that the progression of nutritional deterioration between wasting compartments is insufficient to maintain persistent amplification of undernutrition prevalence within the population. As a consequence, both moderate and severe wasting prevalence decline progressively over time. However, the simulations further reveal that satisfying the condition $\mathcal{R}_W < 1$ does not necessarily imply complete elimination of undernutrition. Moderate wasting, severe wasting, and stunting all remain strictly positive at equilibrium, although at substantially reduced levels. Therefore, the system converges toward a stable low-endemic equilibrium rather than toward a completely undernutrition-free state.

This distinction is epidemiologically important because it indicates that undernutrition remains structurally embedded within vulnerable subpopulations despite the suppression of wasting progression dynamics. Persistent low-level prevalence may continue to arise from long-term socioeconomic deprivation, maternal malnutrition, household food insecurity, recurrent infections, poor sanitation, and other environmental risk factors that are not fully removed from the population. Consequently, although the condition $\mathcal{R}_W < 1$ guarantees long-term dynamical stability and substantial reductions in wasting prevalence, sustainable elimination of childhood undernutrition still requires continuous integrated interventions targeting both acute nutritional deterioration pathways and broader structural determinants of chronic malnutrition.

The simulation outcomes are also highly consistent with the sensitivity analysis results obtained previously. The sensitivity analysis identified deterioration-related parameters associated with nutritional progression pathways as dominant positive contributors to

undernutrition persistence, whereas recovery-related parameters exerted strong negative influence on the system by suppressing wasting progression dynamics. These theoretical findings are directly reflected in the numerical simulations shown in Figure 4. The rapid reduction in severe wasting prevalence indicates that recovery mechanisms dominate deterioration pathways under the calibrated parameter regime, while the persistence of low-level moderate wasting and stunting indicates that deterioration pathways remain active, although substantially weakened.

Furthermore, the very small estimated value of \mathcal{R}_W suggests that recovery-related processes strongly outweigh the deterioration parameters governing wasting transmission dynamics. Consequently, the system becomes highly stable and resistant to sustained growth in wasting prevalence. Nevertheless, the sensitivity analysis also implies that relatively small increases in deterioration-related parameters may substantially alter the long-term equilibrium structure. For example, increases in nutritional deterioration rates associated with food insecurity, recurrent infections, economic crises, or inadequate healthcare access may elevate wasting prevalence and potentially shift the system toward a less favorable endemic regime. Similarly, reductions in recovery-related mechanisms caused by weakened intervention programs or declining healthcare coverage may increase the effective value of \mathcal{R}_W , thereby destabilizing the low-endemic equilibrium observed in the present simulations.

From a public health perspective, the projections provide several important implications. First, the rapid decline in severe wasting indicates that intensive nutritional treatment programs and recovery-oriented interventions can substantially reduce severe acute malnutrition over the long term. Second, the persistence of moderate wasting and stunting despite $\mathcal{R}_W < 1$ suggests that treatment-oriented interventions alone are insufficient to completely eliminate undernutrition. Chronic nutritional problems remain structurally embedded within vulnerable populations because of persistent socioeconomic and environmental determinants. Therefore, sustainable reductions in childhood undernutrition require integrated long-term strategies combining acute wasting treatment with broader interventions targeting maternal nutrition improvement, sanitation enhancement, infection prevention, food security strengthening, poverty reduction, and optimal childcare practices.

Overall, Figure 4 demonstrates that the wasting–stunting system possesses dynamically stable long-term behavior under the calibrated parameter regime. The threshold condition $\mathcal{R}_W < 1$, the local stability analysis, the sensitivity analysis, and the numerical projections consistently indicate that the system converges toward a stable low-endemic equilibrium characterized by declining undernutrition prevalence and increasing dominance of the well-nourished population. Nevertheless, the persistence of positive equilibrium levels demonstrates that undernutrition remains structurally sustained within vulnerable groups, emphasizing the necessity of maintaining continuous and integrated nutritional intervention policies over the long term.

E. CONCLUSION AND SUGGESTIONS

This study develops a deterministic compartmental model describing the interaction between wasting and stunting among children under five years of age by incorporating wasting progression, direct pathways toward stunting, and age-dependent recovery dynamics within a

unified mathematical framework. Model calibration using Indonesian national prevalence data during 2013–2024 produced a residual error of approximately 8.77×10^{-3} , indicating good agreement between simulated trajectories and observed prevalence data. Numerical simulations show declining trends for severe wasting, whereas stunting decreases more slowly and remains relatively persistent over time. The estimated recovery parameters further indicate that infants recover faster than older children, supporting the biological assumption underlying the proposed age-dependent recovery mechanism.

Threshold and local stability analysis demonstrate that the condition $\mathcal{R}_W < 1$ is associated with decay of wasting dynamics and convergence toward equilibrium. However, sensitivity analysis indicates that long-term stunting dynamics are influenced more strongly by deterioration and progression pathways toward stunting than by recovery mechanisms. In particular, the deterioration rate toward moderate wasting exhibited the highest sensitivity influence, indicating that early nutritional deterioration plays a dominant role in shaping long-term stunting prevalence. In contrast, infant-related recovery parameters exhibit comparatively low sensitivity influence, suggesting that recovery improvement alone may not substantially reduce long-term stunting prevalence at the population level.

These findings suggest that reducing wasting alone may not be sufficient to substantially lower long-term stunting prevalence. Sustainable stunting reduction therefore requires integrated interventions addressing both acute and chronic undernutrition pathways, including maternal nutrition improvement, infant feeding optimization, sanitation enhancement, infection prevention, household food security, and continuous nutritional monitoring during the first 1000 days of life. This study still has several limitations. The model is calibrated using aggregated annual prevalence data and does not explicitly capture individual-level heterogeneity, spatial variability, or stochastic fluctuations. In addition, concurrent wasting–stunting is represented implicitly rather than through a separate compartment due to limited longitudinal data availability. Future studies may extend the present framework by incorporating stochastic effects, spatial heterogeneity, longitudinal cohort data, or explicit concurrent wasting–stunting compartments to obtain a more comprehensive representation of undernutrition dynamics

ACKNOWLEDGEMENT

The authors gratefully acknowledge financial support from the Direktorat Penelitian dan Pengabdian kepada Masyarakat (DPPM), Ministry of Higher Education, Science, and Technology of the Republic of Indonesia, through the Program Penelitian Dosen Pemula (PDP) under Contract Number 020/IT13.D/KH-DPPM/2025, Fiscal Year 2025.

REFERENCES

- Aisyah, I. S., Khomsan, A., Tanziha, I., & Riyadi, H. (2024). A multiple logistic regression analysis of household food and nutrition insecurity in stunting and non-stunting toddlers. *Current Research in Nutrition and Food Science*, 12(1), 452–461. <https://doi.org/10.12944/CRNFSJ.12.1.36>
- Avalos, D., Cuadrado, C., Dunstan, J., Moraga-Correa, J., Rojo-González, L., Troncoso, N., & Vásquez, Ó. C. (2021). Mathematical model for estimating nutritional status of the population with poor data quality in developing countries: The case of Chile. *The 10th International Conference on Operations Research and Enterprise Systems (ICORES 2021)*, 408–415. <https://doi.org/10.5220/0010262404080415>

- Badan Kebijakan Pembangunan Kesehatan (BKPK) Kementerian Kesehatan Republik Indonesia. (2024). *Survei Kesehatan Indonesia (SKI) Tahun 2023*. Kemenkes BKPK.
- Badan Penelitian dan Pengembangan Kesehatan. (2019). *Laporan Nasional RISKESDAS 2018*.
- Bahagia Febriani, A. D., Daud, D., Rauf, S., Nawing, H. D., Ganda, I. J., Salekede, S. B., Angriani, H., Maddeppungeng, M., Juliaty, A., Alasiry, E., Artaty, R. D., Lawang, S. A., Ridha, N. R., Laompo, A., Rahimi, R., Aras, J., & Sarmila, B. (2020). Risk factors and nutritional profiles associated with stunting in children. *Pediatric Gastroenterology, Hepatology and Nutrition*, 23(5), 457–463. <https://doi.org/10.5223/PGHN.2020.23.5.457>
- Damanik, H. D. L., Flora, R., Zulkifli, H., & Zulkarnain, M. (2025). Exclusive Breastfeeding and Educational Attainment of Mother Correlate with Stunting Problem in Musi Rawas Regency. *Jurnal Promkes: The Indonesian Journal of Health Promotion and Health Education*, 13(1), 147–154. <https://doi.org/10.20473/jpk.V13.I1SI.2025.147-154>
- De Onis, M., & Branca, F. (2016). Childhood stunting: a global perspective. *Maternal & Child Nutrition*, 12, 12–26. <https://doi.org/10.1111/mcn.12231>
- Fikri, A. A., & Komalyna, I. N. T. (2023). Risk Factors Affecting Stunting of Toddlers in Murtajih Village, Pamekasan District. *Media Gizi Indonesia*, 18(1), 49–55. <https://doi.org/10.20473/mgi.v18i1.49-55>
- Hamid, S. B. A., Denil, N. M., Ismail, N. A., & Mauludyani, A. V. R. (2024). Stunting and food insecurity among children from low socioeconomic family during COVID-19 pandemic in urban area in Selangor. *Medical Journal of Malaysia*, 79, 53–58. <https://pubmed.ncbi.nlm.nih.gov/38555886/>
- Harper, A., Rothberg, A., Chirwa, E., Sambu, W., & Mall, S. (2023). Household Food Insecurity and Demographic Factors, Low Birth Weight and Stunting in Early Childhood: Findings from a Longitudinal Study in South Africa. *Maternal and Child Health Journal*, 27(1), 59–69. <https://doi.org/10.1007/s10995-022-03555-7>
- Harper, K. M., Mutasa, M., Prendergast, A. J., Humphrey, J., & Manges, A. R. (2018). Environmental enteric dysfunction pathways and child stunting: A systematic review. *PLoS Neglected Tropical Diseases*, 12(1), 1–23. <https://doi.org/10.1371/journal.pntd.0006205>
- Himmah, E. F., Kaestria, R., & Riana. (2025). Mathematical Modeling of Stunting with the Influence of Nutritional Intervention. *JTAM (Jurnal Teori Dan Aplikasi Matematika)*, 9(1), 54–67. <https://doi.org/10.31764/jtam.v9i1.26817>
- Indahsari, N. K., Herliani, O., & Masfufatun, M. (2023). The relationship between food quantity and diversity with stunting incidence in Indonesia. *Healthcare in Low-Resource Settings*, 11(2), 251–258. <https://doi.org/10.4081/hls.2023.11773>
- Jokhu, L. A., & Syauqy, A. (2024). Determinants of concurrent wasting and stunting among children 6 to 23 mo in Indonesia. *Nutrition*, 122(112390), 1–7. <https://doi.org/10.1016/j.nut.2024.112390>
- Kementerian Kesehatan Republik Indonesia. (2013). *Profil Kesehatan Indonesia Tahun 2013*.
- Kementerian Kesehatan Republik Indonesia. (2016). *Profil Kesehatan Indonesia Tahun 2015*.
- Kementerian Kesehatan Republik Indonesia. (2017). *Profil Kesehatan Indonesia tahun 2016*.
- Kementerian Kesehatan Republik Indonesia. (2018). *Profil Kesehatan Indonesia Tahun 2017*.
- Kementerian Kesehatan Republik Indonesia. (2019). *Profil Kesehatan Indonesia Tahun 2018*.
- Kementerian Kesehatan Republik Indonesia. (2022). *Profil Kesehatan Indonesia 2022*.
- Kementerian Kesehatan Republik Indonesia. (2023). *Hasil Survei Status Gizi Indonesia 2022*.
- Kementerian Kesehatan Republik Indonesia. (2024). *Profil Kesehatan Indonesia Tahun 2023*.
- Kementerian Kesehatan Republik Indonesia. (2025a). *Profil Kesehatan Indonesia Tahun 2024*.
- Kementerian Kesehatan Republik Indonesia. (2025b). *SSGI 2024: Survei Status Gizi Indonesia dalam angka*.
- Masitoh, S., Nurokhmah, S., & Ronoatmodjo, S. (2023). The Correlation Between Food Insecurity Level and Stunting in Indonesia. *Jurnal Ilmu Kesehatan Masyarakat*, 13(3), 385–398. <https://doi.org/10.26553/jikm.2022.13.2.385-398>
- Meisel, J. D., Sarmiento, O. L., Olaya, C., Lemoine, P. D., Valdivia, J. A., & Zarama, R. (2018). Towards a novel model for studying the nutritional stage dynamics of the Colombian population by age and socioeconomic status. *PLoS ONE*, 13(2), 1–22. <https://doi.org/10.1371/journal.pone.0191929>
- Mertens, A., Benjamin-Chung, J., Colford, J. M., Hubbard, A. E., van der Laan, M. J., Coyle, J., Sofrygin, O., Cai, W., Jilek, W., Rosete, S., Nguyen, A., Pokpongkiat, N. N., Djajadi, S., Seth, A., Jung, E., Chung, E.

- O., Malenica, I., Hejazi, N., Li, H., ... Yori, P. P. (2023). Child wasting and concurrent stunting in low- and middle-income countries. *Nature*, 621(7979), 558–567. <https://doi.org/10.1038/s41586-023-06480-z>
- Millward, D. J. (2017). Nutrition, infection and stunting: The roles of deficiencies of individual nutrients and foods, and of inflammation, as determinants of reduced linear growth of children. *Nutrition Research Reviews*, 30(1), 50–72. <https://doi.org/10.1017/S0954422416000238>
- Murni, I. K., Patmasari, L., Wirawan, M. T., Arafuri, N., Nurani, N., Sativa, E. R., Nugroho, S., & Noormanto. (2023). Outcome and factors associated with undernutrition among children with congenital heart disease. *PLoS ONE*, 18(2), 1–10. <https://doi.org/10.1371/journal.pone.0281753>
- Nomura, K., Bhandari, A. K. C., Matsumoto-Takahashi, E. L. A., & Takahashi, O. (2023). Risk factors associated with stunting among children under five in Timor-Leste. *Annals of Global Health*, 89(1:63), 1–14. <https://doi.org/10.5334/aogh.4199>
- Permatasari, R. P., Simbolon, D., & Yunita, Y. (2024). Stunting Prevention through Exclusive Breastfeeding in Indonesia: A Meta-Analysis Approach. *Amerta Nutrition*, 8(1SP), 105–112. <https://doi.org/10.20473/amnt.v8i1SP.2024.105-112>
- Rahmi, N., & Ekasasmita, W. (2024). A mathematical model to restrain pneumonia spread in children under five years considering nutritional status, household air pollution, vaccination, and health monitoring. *The 6th IICMA 2023*, 58, 1–14. <https://doi.org/https://doi.org/10.1051/itmconf/20245801001>
- Schoenbuchner, S. M., Dolan, C., Mwangome, M., Hall, A., Richard, S. A., Wells, J. C., Khara, T., Sonko, B., Prentice, A. M., & Moore, S. E. (2019). The relationship between wasting and stunting: A retrospective cohort analysis of longitudinal data in Gambian children from 1976 to 2016. *American Journal of Clinical Nutrition*, 110(2), 498–507. <https://doi.org/10.1093/ajcn/nqy326>
- Singh, A., Singh, A., & Ram, F. (2014). Household food insecurity and nutritional status of children and women in Nepal. *Food and Nutrition Bulletin*, 35(1), 3–11. <https://doi.org/10.1177/156482651403500101>
- Tello, B., Rivadeneira, M. F., Moncayo, A. L., Buitrón, J., Astudillo, F., Estrella, A., & Torres, A. L. (2022). Breastfeeding, feeding practices and stunting in indigenous Ecuadorians under 2 years of age. *International Breastfeeding Journal*, 17(1), 1–15. <https://doi.org/10.1186/s13006-022-00461-0>
- UNICEF/WHO/World Bank Group. (2025). *Levels and trends in child malnutrition: UNICEF/WHO/World Bank Group joint child malnutrition estimates: Key findings of the 2025 edition*.
- Wicaksono, R. A., Arto, K. S., Mutiara, E., Deliana, M., Lubis, M., & Batubara, J. R. L. (2021). Risk factors of stunting in Indonesian children aged 1 to 60 months. *Paediatrica Indonesiana(Paediatrica Indonesiana)*, 61(1), 12–19. <https://doi.org/10.14238/pi61.1.2021.12-9>
- Winarni, A., Sofiyati, N., & Rudatiningtyas, U. F. (2024). Analysis and Simulation of SEIR Mathematical Model of Stunting Case in Indonesia. *Mathline: Jurnal Matematika dan Pendidikan Matematika*, 9(3), 871–886. <https://doi.org/10.31943/mathline.v9i3.555>